We are IntechOpen,
the world's leading publisher of
Open Access books
Built by scientists, for scientists

6,900
Open access books available

186,000
International authors and editors

200M
Downloads

154
Countries delivered to

Our authors are among the
TOP 1%
most cited scientists

12.2%
Contributors from top 500 universities

WEB OF SCIENCE™
Selection of our books indexed in the Book Citation Index
in Web of Science™ Core Collection (BKCI)

Interested in publishing with us?
Contact book.department@intechopen.com

Numbers displayed above are based on latest data collected.
For more information visit www.intechopen.com

Chapter 7

Polymeric Prosthesis as Acoustic, Pressure, Temperature, and Light Sensor Fabricated by Three-Dimensional Printing

Ernesto Suaste-Gómez, Grissel Rodríguez-Roldán,
Héctor Reyes-Cruz and Omar Terán-Jiménez

Additional information is available at the end of the chapter

http://dx.doi.org/10.5772/63074

Abstract

There have been new developments in prosthetic technology over the past 30 years, and the union of bionics and prosthetics has improved mobility and aesthetics, however, a person who lacks a limb will have to continue without a valuable sense, touch. As a result of stimulation of the receptors under the skin and subcutaneous tissue, touch is sensitive to mechanical stimuli and stimuli that produce heat, cold, and pain. In this chapter, the results presented include the stages of design, construction, and characterization of an ear prosthesis manufactured with a 3D printer in polyvinylidene fluoride (PVDF), which is a biocompatible and ferroelectric smart material (exhibits piezoelectric and pyroelectric properties). Thus, the behavior of the prosthesis in response to external stimuli such as pressure, heat, cold, acoustic waves, and light is presented, thereby, extending the purpose of a prosthesis to the area of sensory perception.

Keywords: Piezoelectric, photopyroelectric, polymer, 3D printer, pressure, prostheses, PVDF, smart materials, temperature

1. Introduction

Recent advances in bionics and prosthetics have combined different techniques to develop; in the last few years, aesthetic and functional prostheses which allow people with physical disabilities caused either by an accident or by a genetic deformity to get on with their life.

INTECH
open science | open minds

© 2016 The Author(s). Licensee InTech. This chapter is distributed under the terms of the Creative Commons Attribution License (http://creativecommons.org/licenses/by/3.0), which permits unrestricted use, distribution, and reproduction in any medium, provided the original work is properly cited.

Ear prostheses (which in common parlance are called "artificial ear") are an example of progress in this area. They are commonly used in patients with microtia, which is a congenital malformation characterized by the underdevelopment of an ear or two and which is usually broken down into four categories:

- Grade I is a slightly small ear with identifiable structures and a small but present external ear canal.
- Grade II is a partially formed ear, usually with a closed off or stenotic external ear canal producing a conductive hearing loss.
- Grade III is the absence of the external ear with a small "peanut" skin and cartilage structure and the absence of the external ear canal and ear drum.
- Grade IV is absence of the total ear (anotia).

In addition to the psychologic effect of a grossly deformed ear, the child or adult with microtia has moderate to severe conductive hearing loss. Although those patients have a normal inner ear, it is frequently observed an absence of the external ear (or pinna), an absent external canal and ear drum as well as a smaller middle ear cavity, fused middle ear bones (ossicles), and an open (patent) eustachian tube. Therefore, these patients have a maximum conductive hearing loss. Because it is critical for these patients to have normal hearing in order to have normal speech and bilateral hearing in order to detect directionality, ear prostheses have become the most recommendable alternative, allowing the patient to recover both functionality and appearance of a natural ear [1].

This chapter will present the results including the stages of design, fabrication, and characterization of a 3D-printed ear prosthesis using PVDF, a polymeric smart material which is used as either a sensor or a transducer due to its high piezoelectric, pyroelectric, photopyroelectric, and ferroelectric properties [2–6].

PVDF is the most significant and studied polymer by Lovinger, "Ferroelectric Polymers" in *Science*, 1983 [7] and Gallantree "Review of transducer applications of polyvinylidene fluoride" 1983 [3]; PVDF responds to pressure (piezoelectric effect), temperature, sound, light, and even moisture (reported by our group), "System for Controlling Moisture of the Soil Using Humidity Sensors from a Polyvinylidene fluoride Fiber mats" [8]. Other polymeric materials which are not pure and exhibit these properties are ZnO/PVDF with graphene for pressure and temperature sensing, described by Lee et al. 2015 [5] or the compounds mentioned in **Table 3** "Comparison of piezoelectric properties of some semicrystalline polymeric material" in *Piezoelectric Polymers*, 2001 [9].

The prosthesis was subjected to pressure, temperature, light, and acoustic stimuli. Thus, the response of these stimuli is presented. This way it is expected to restore sensory function, giving the user the ability to perceive heat, cold, touch, and pressure ae did before as well as acoustic waves and light.

http://dx.doi.org/10.5772/63074

2. Experimental section

2.1. Design and manufacturing

An ear prosthesis was created according to anthropometric parameters. It was designed using a 3D computer-aided design (CAD) software. After that, the prosthesis was manufactured with a 3D printer from bits from bytes, model 3D touch with a Z-axis resolution of 0.125 mm (0.005″/ 125 microns), nozzle has a diameter of 0.3 mm, using the fused deposition modeling (FDM) process and printed in PVDF ($C_2H_2F_2$) which is a smart material that exhibits piezoelectric and pyroelectric properties. PVDF used was pure and bought in rods with 3 mm of diameter, from Goodfellow Limited Cambridge (FV307910), and this PVDF is subjected to strict quality control to assure repeatability in its ferroelectric properties, that is, piezoelectric and pyroelectric properties of the printed ear are not affected.

Types of 3D printers:

- Stereolithography (SLA)
- Fused deposition modeling (FDM)
- Selective laser sintering (SLS)
- Selective laser melting (SLM)
- Electronic beam melting (EBM)
- Laminobject manufacturing (LOM)

2.2. Polarization

PVDF is polymorphic and has a crystalline phase (ß-phase). The ß-phase is the most relevant phase for practical ferroelectric, piezoelectric, and pyroelectric applications. Several methods are commonly used in order to achieve this phase, such as stretching the material, applying a voltage of at least 0.5 MV/cm, or using plasma or corona poling [7].

The ear prosthesis made of PVDF was poled by corona poling, where a high voltage (15 kV) was applied between a needle and a plate, situated 1 cm apart. PVDF prosthesis was placed over the plate, so the molecules of this polymer are aligned [7, 10].

2.3. Characterization

In this stage, the ear prosthesis was characterized by means of applying different stimuli such as pressure, heat, and cold (imitating human skin receptors) and also acoustic waves and light, that is, temperature, sound, pressure, and light (TSPL) stimuli, in order to register different responses of the PVDF prosthesis as a multisensory unit. **Figure 1** shows the general diagram of the experiments that are mentioned above.

Figure 1. Diagram of different applied stimuli TSPL to the PVDF prosthesis.

2.3.1. Hysteresis loop

In order to measure ferroelectric hysteresis loop, the Sawyer–Tower circuit was implemented for this study (**Figure 2**). By measuring voltage (V_L) across a capacitor (C_L = 0.15 μF) in series with the PVDF prosthesis (C_F), the charge on the ferroelectric can be determined since $Q_F = C_L \times V_L$. A sine wave was applied to the circuit with a function generator, Rigol model DG4062; X channel was measured from an X–Y trace using an oscilloscope, Tektronix model MSO 3014.

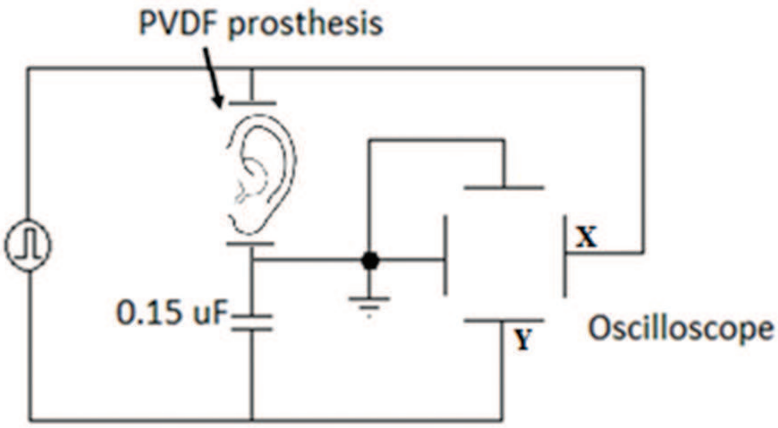

Figure 2. Measure of ferroelectric hysteresis loop using the Sawyer–Tower circuit.

2.3.2. Acoustic response

In this experiment, a sound source was used as a sound emitter (a) excited by an audio generator at 60 Hz. As the receiver, it was used a face of the PVDF prosthesis which was

http://dx.doi.org/10.5772/63074

metalized (mirror finish) (b) by in situ thermal evaporation of aluminum in a vacuum chamber at 10^{-4} mmHg. A sound source was situated 5 mm from the speaker; at the same time, it was reflected a red laser beam of helium–neon at 633 nm, JDSU model 1145AP (c) which is detected by a light detector, light-to-frequency converter TSL230 from Texas Instruments (d); thus obtaining two electric signals, one from PVDF and another from the light detector in the oscilloscope, Tektronix model MSO3014, (e) displayed. **Figure 3** shows a schematic diagram of the experiment mentioned above.

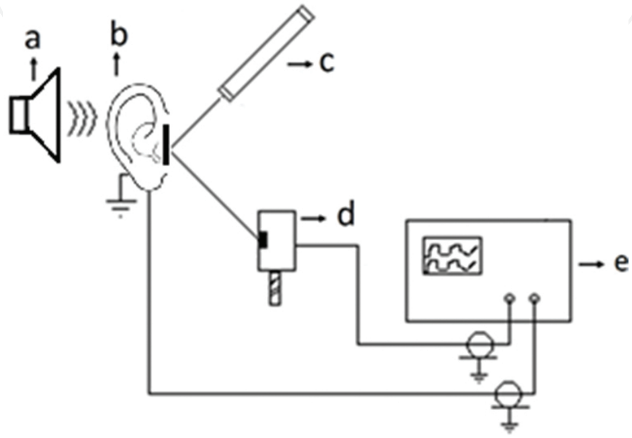

Figure 3. (a) Sound source, (b) section of PVDF (mirror finish), (c) laser HeNe 633 nm, (d) light detector, and (e) oscilloscope.

2.3.3. Photopyroelectric response

The interest of recording photopyroelectric current (Y-axis) is to show that the PVDF used in the manufacture of hearing aid responds to light, PVDF was stimulated with a modulated laser light (electronically chopped by the internal oscillator) with a maximum power of 150 mW through an optical fiber with a wave length λ of 650 nm (laser BWTEK model BWF-650-15E/55369). Two frequency sweeps were carried out, one from 0 to 10 Hz and the other from 0 to 100 Hz [frequency (X-axis)] were used. This experimental arrangement is based on Balderas-Lopez and Mandelis "New Technique for Precise Measurements of the thermal Effusivity of Transparent Liquids," 2003 [11] and Mandelis and Wang "A Novel PVDF Thin-Film Photopyroelectric Thermal-Wave Interferometry," 2000 [12]. Our group have compared and discussed the use of PVDF with the ferroelectric ceramic PLZT as a pyroelectric sensor, "Comparative performance of PLZT and PVDF Sensors Used Phyroelectric to the Thermal Characterization of Liquid Samples," 2013 [13].

In order to evaluate photopyroelectric response of the printed PVDF, the experimental arrangement of **Figure 4** was done. The printed PDVF prosthesis (c) was excited with a laser system, BWTEK model BWF-650-15E/55369 λ = 650 nm (e). The laser beam was modulated under two ranges: from 0 to 100 Hz and from 0 to 10 Hz. The intensity of the laser is a function of the emitter current. To register the photopyroelectric response of the printed PVDF prosthesis, a current preamplifier, Standford Research Systems model SR570 and an oscilloscope, Tektronix model MSO3014, were used.

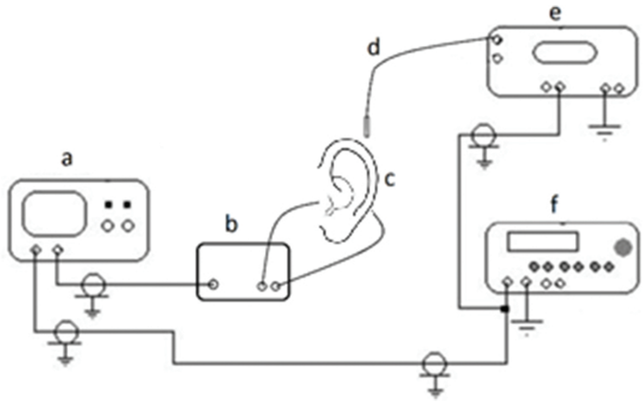

Figure 4. Experimental arrangement of the photopyroelectric response of printed PVDF. (a) Oscilloscope, (b) current preamplifier, (c) printed PVDF prosthesis, (d) fiber optic, (e) laser system, and (f) function generator.

2.3.4. Pressure and temperature characterization

The prosthesis was tested as a pressure sensor with different pressure loads between 0 and 16.35 kPa using a certified weight set from OHAUS. The prosthesis was set in horizontal position, and weights between 25 g and 3 kg were placed over the printed ear as shown in **Figure 5**.

Figure 5. Example of pressure characterization.

From Newton's second law (Eq. 1), we have a relation between force (F) and mass (m).

http://dx.doi.org/10.5772/63074

$$f = ma \tag{1}$$

where

F = force (N)

m = mass (kg)

a = 9.81 m/s^2

Equation (2) was used in order to determine the pressure generated over the ear prosthesis.

$$P = \frac{F}{A} \tag{2}$$

where

F = force (N)

A = area of the surface of the ear on contact with the weights (m^2).

Regarding to temperature characterization, it has been performed laying the ear prosthesis in an ice bath from 5 to 25°C and in a chamber furnace from 25 to 90°C (in 5°C intervals). The characterization of temperature was done up to 150°C; however, responses between 90° and 150°C remained unchanged, and a fact that was preliminary confirmed by Davis in "Piezoelectric and Pyroelectric Polymers," 1993 [14] who recommends that the maximum temperature of operation of the PVDF must be 80°C (melting point of around 177°C) [14]. Moreover, for the ear prosthesis of PVDF, the temperature response is in the range of normal temperature of human be [36.19°C (97°F) to 37.2°C (99°F)].

Concerning low temperatures (under 0°C), our research group tested the response of the 3D printed ear (poled and unpoled) at temperatures from −160 to 5°C, giving as a result a minimum temperature of −43.15°C for the unpoled prosthesis and −47 for the poled prosthesis. In this context, manufacturers of PVDF reported the minimum operating temperature at −35°C. It has been also reported in the literature and technical notes that PVDF has a glass transition temperature (Tg) of about −35°C where PVDF is typically 50–60% crystalline and the lowest operating temperature is −50°C (Hylar® Kynar®).

Moreover, PVDF can be used at temperatures from −80° to 300°F (−62° to 149°C). Polyvinylidene fluoride (PVDF) is a fluorocarbon classified as "self-extinguishing, group 1" Underwriters Laboratories, Inc. It is not affected by prolonged exposure to sunlight or other sources of ultraviolet radiation. It retains its properties under high vacuum and gamma radiation, and it is also resistant to most acids and alkalis (Porex Corporation). Additionally, the company Boveag indicates a temperature range of −30 to 150°C. Goodfellow reports thermal properties of PVDF, minimum operating temperature: −40°C, and maximum operating temperature: 135–150°C.

The basic circuit used for detecting pressure and temperature of the PVDF prosthesis is shown in **Figure 6**. The circuit is a relaxation oscillator (Astable Circuit Operation LM555, Texas instrument). Changes in PVDF prosthesis capacitance are observed according to the variations in temperature and pressure.

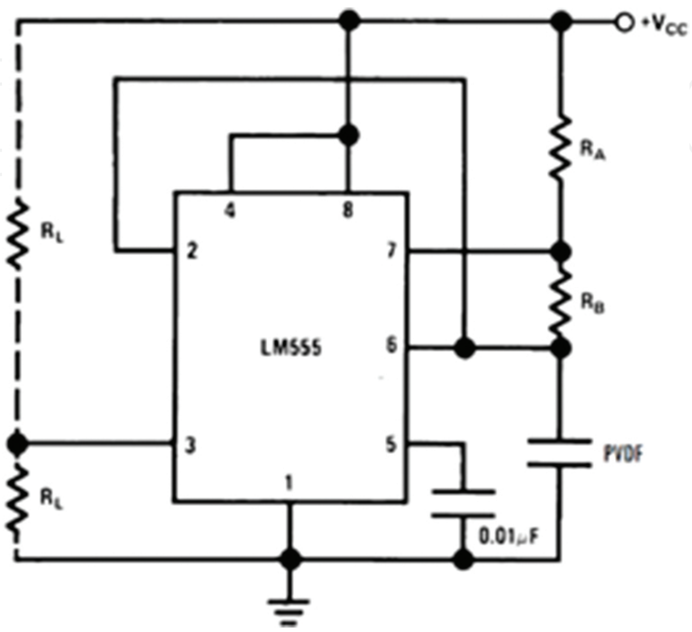

Figure 6. Astable multivibrator circuit LM555 to register changes of temperature and pressure of the PVDF prosthesis.

The circuit shown in **Figure 6** generates a clock signal, where the frequency of oscillation depends on 2 resistors, RA, RB, and one capacitor, C, as shown in Eq. (3). Instead of C, the PVDF prosthesis was set and the frequency response was observed.

$$f = \frac{1.44}{(RA + 2RB)C} \tag{3}$$

We have also used the circuit of **Figure 6** as a moisture sensor [8]. Moreover, pressure and temperature measurements were done to 3D-printed PVDF samples (FV307910), noting that if thickness and/or dimensions change, the response also changes but the trend still remains. This is clearly explained by the Eq. (4):

$$C = \frac{\varepsilon_r \varepsilon_0 A}{d} \tag{4}$$

where C is the capacitance, ε_r is the relative permittivity of the dielectric, ε_0 is the vacuum permittivity ($\varepsilon_0 = 8.854 \times 10^{-12}$ F/m), A is the area of the PVDF or capacitor plates, and d is the PVDF thickness or the distance between the electrodes or plates (see Equation (5) of Ref. [16]).

Equation (4) describes the relationship between permittivity, capacity, and physical dimensions of the ferroelectric PVDF when it is subjected to pressure (see standard weights **Figure 5**) or it is deformed see **Figure 3** article our group "Polyvinylidene Flouride in an Applied Polymer Intraocular Pressure Sensor," 2005 [6].

Thermal behavior of PVDF dielectric response changes can be widely seen in the following articles: Casar et al. "Electrical and thermal properties of vinylidene fluoride–trifluoroethylene-based polymer System with coexisting ferroelectric and relaxor states," 2013 [15]; Jafer et al. "The Use of PE/PVDF Pressure and Temperature Sensors in Smart Wireless Sensor Network for Environmental Monitoring System Developed," 2008 [16]. And Jia et al. "Simulation and Experiment of PVDF temperature sensor," 2013 [17].

Finally, using Eqs. (3) and (4), the frequency of the circuit LM555 where PVDF was set instead of C is; we have, 1.44/(RA + 2RB) $f = (\varepsilon_r \varepsilon_0 A)/d$; where

$$f = \frac{(1.44)\mathrm{d}}{\varepsilon_r \varepsilon_0 A(\mathrm{RA} + 2\mathrm{RB})} \tag{5}$$

Demonstrating that any alteration of PVDF in its intrinsic permittivity and/or physical dimensions changes *f* by action of pressure and temperature in the ear made with PVDF shown in the following results of **Figure 7** (*f* vs. P) and **Figure 8** (*f* vs. T). Incidentally by a frequency-to-voltage converter may be plotting voltage vs. pressure or temperature.

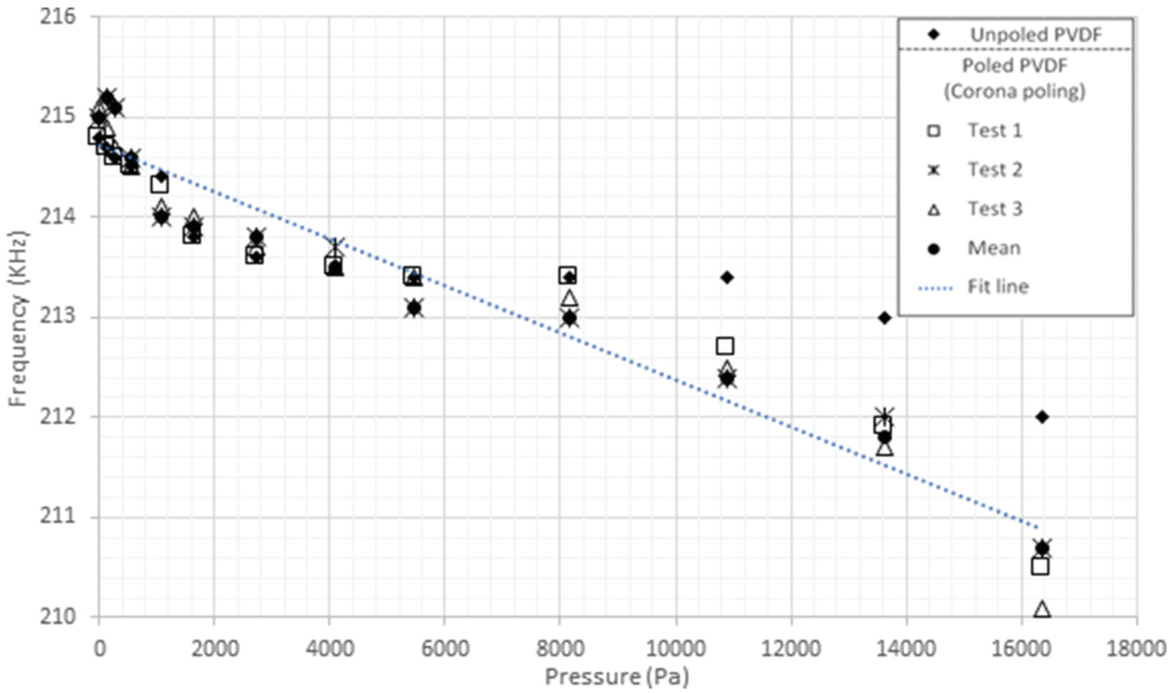

Figure 7. Response of the prosthesis of PVDF as a pressure sensor from 0 to 16350 Pa.

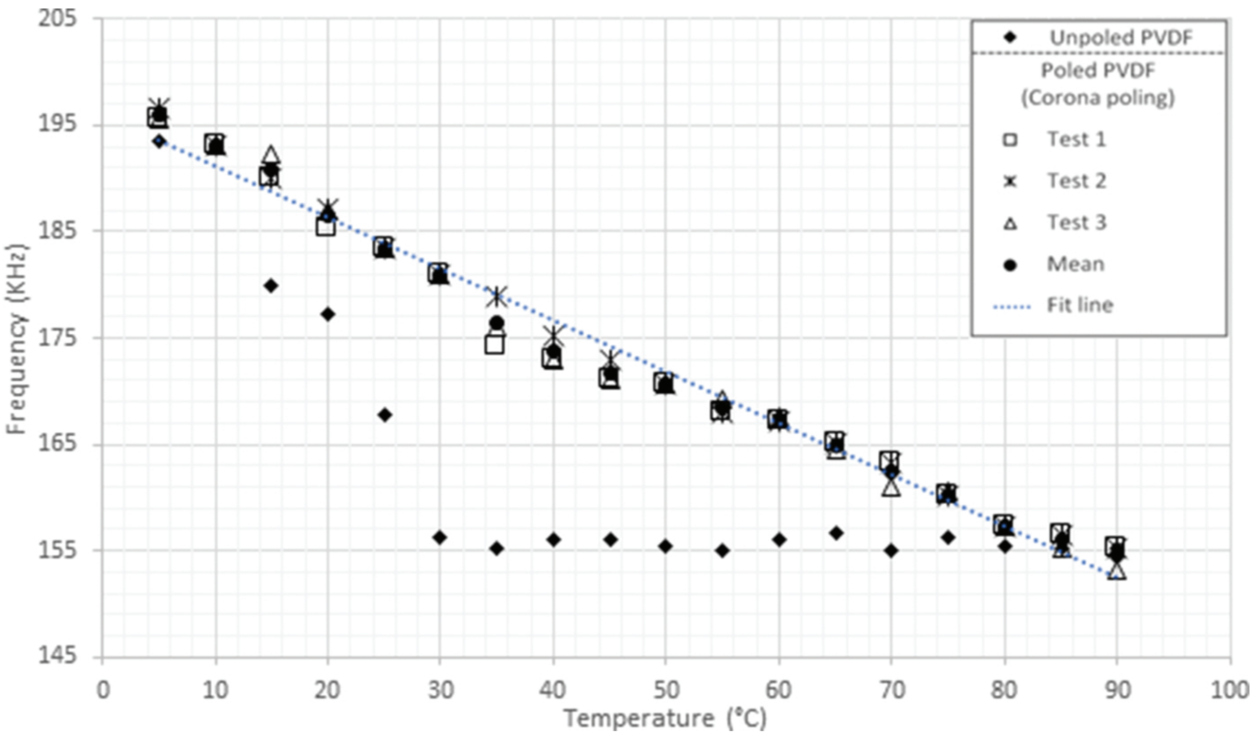

Figure 8. Thermal responses of prostheses made of PVDF from 2 to 90°C.

3. Results

Figure 9a shows the design of a 3D human ear model according to anthropometric parameters [18–20] and created with a computer-aided design (CAD) software. It was exported as a stereolithography file in order to print it using a 3D printer.

IntechOpen

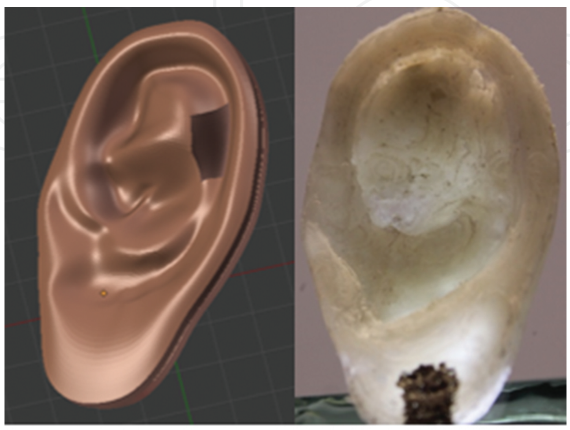

a) b)

Figure 9. (a) Human ear created with a 3D CAD program. (b) Ear prosthesis printed of PVDF.

http://dx.doi.org/10.5772/63074

The ear was printed in polyvinylidene fluoride as it exhibits ferroelectric properties. **Figure 9b** shows the 3D-printed ear prosthesis. The dimensions of the printed ear are 60.1 mm wide by 34.74 mm long and has an average thickness of 6.88 mm. Electrodes were painted over the printed ear with silver paint from SPI Supplies. The area of these electrodes is 6.26 mm^2, and the distance between them is 41 mm (**Figure 10**). Dimensions were measured with a Starrett Vernier with 0.02 mm precision.

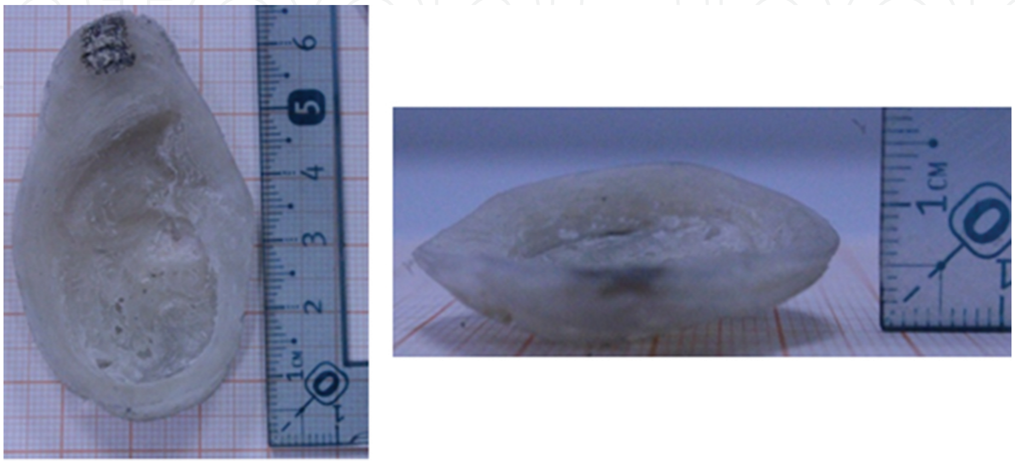

Figure 10. Dimensions of ear prosthesis printed of PVDF.

Sawyer–Tower circuit (**Figure 2**) was used to measure ferroelectric properties such as hysteresis. **Figure 11** shows P–E hysteresis loop of the printed PVDF, and X axis shows the electric field (E) in kV/cm and Y axis polarization (P) in $\mu C/cm^2$.

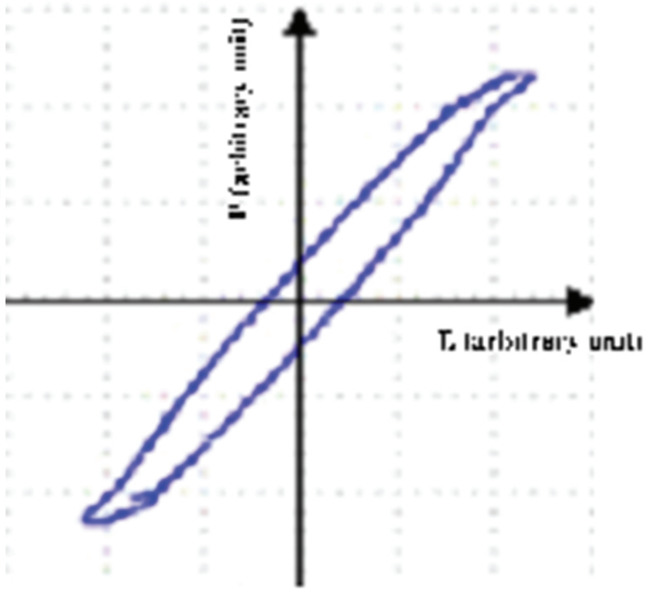

Figure 11. Printed PVDF hysteresis loop.

The acoustic response using a metalized printed PVDF sample is presented in **Figure 12**. The electrical signal from the light detector was recorded after PVDF reflected the laser beam. Variations of the laser intensity correspond to fluctuations of amplitude and frequency in the electrical signal.

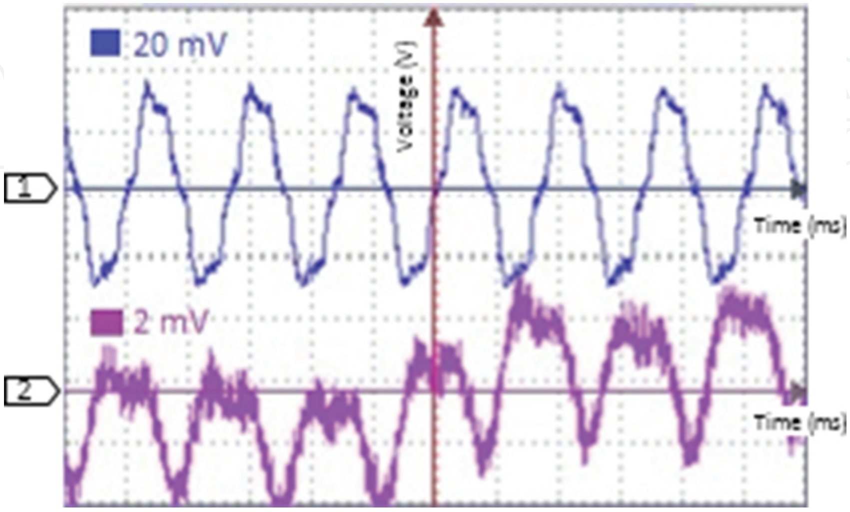

Figure 12. Reference signal for printed PVDF (Ch1) and the signal obtained from a commercial light detector (Ch2).

Results of photopyroelectric response of printed PVDF prosthesis at 10 and 100 Hz are shown in **Figure 13a, b**, respectively.

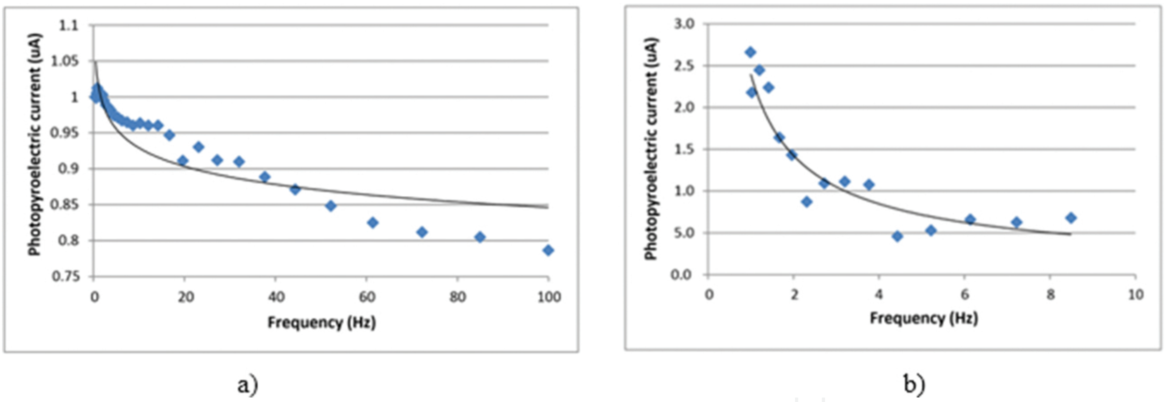

Figure 13. (a) Printed PVDF sample photopyroelectric response (100 Hz), (b) printed PVDF sample photopyroelectric response (10 Hz).

The results in **Figure 13a, b** showed an asymptotic behavior, similar to the ones described in the theory in the case of frequency modulation of laser stimulation. References amply illustrate the use of PVDF in the photopyroelectric technique [11–13].

The prosthesis was also tested as a pressure sensor, applying pressure loads between 0 and 16.35 kPa.

With regard to the characterization of PVDF, ß-phase was reached by means of corona poling. **Figures 7** and **8** show the difference between unpoled and poled PVDF (Tests 1, 2, and 3); the average of these three characterizations (mean) and the line adjustment (fit line).

Figure 7 shows the response of the ear prosthesis of PVDF as a pressure sensor using Eq. (3).

Equation (6) fits a line through the points at 0–16,350 Pa for the corona-poled PVDF prosthesis with correlation coefficient of 0.9670.

$$y = -0.4687x + 217.16 \tag{6}$$

The temperature characterization of the ear prosthesis has been performed from 5 to 90°C in 5°C intervals, and **Figure 8** illustrates the response of the PVDF ear prosthesis as a temperature sensor using Eq. (5). After 90°C, no changes were observed as Davis reported [14].

Equation (7) fits a line through the points at 5 and 90°C for corona-poled PVDF prosthesis with correlation coefficient of 0.9940.

$$y = -2.5132x + 199.34 \tag{7}$$

4. Discussion

The fabrication of an ear prosthesis at present has led to restore the functionality of the middle or inner ear with an electronic hearing aid or implant, respectively [21–26], for patient suffering a dysfunction in the mentioned parts of the ear. By the other side, the ear prosthesis developed in this work focuses on aesthetics and the recovery of acoustic functionality involving only the reconstruction of some of the outer and middle ear structures [27–29]. Both kind of prosthesis (electronic and mechanical) had been designed by separate but an active prosthesis, which covers both aesthetic functionality and the electronic hearing aid (in cases where external, middle, and even the inner ear are damaged either by accident or by a congenital malformation) has not been developed so deeply as the first two mentioned above [30]. In this context, our 3D prosthesis is oriented to provide an aesthetic prosthesis with the ability to sense sound waves without the requirement of another kind of sensor like a microphone or membrane that needs to be placed on the patient's as cochlear implants does. PVDF has demonstrated its ability to work as a microphone [3, 31] due to its piezoelectric properties which can be exploited in the proposed 3D-printed prosthesis.

Regarding the light response of PVDF, results (**Figure 13a, b**) showed an asymptotic behavior, coinciding with the one reported in photopyroelectric techniques [11–13].

In the case of the prosthesis as a temperature sensor, it was observed that it works linearly between 5 and 90°C; after this temperature, there are no more variations. The latter consideration has no impact on the use of the prosthesis usually, as the ambient temperature does not exceed these ranges and the direct application of a higher temperature may cause deformation thereof. It has also been reported that the optimum working temperature is 80°C [14].

The experimental results show an almost linear and inversely proportional behavior between the stimuli of pressure (**Figure 7**) and temperature (**Figure 8**) with the frequency response. The repeatability of the results allows to evaluate the PVDF as a reliable material because each stimulus applied (pressure and temperature) was tested in triplicate, thus obtaining results with slight variations but the same trend. The prosthesis tested as a pressure sensor showed effectiveness in the range of 0–16.35 kPa, values that also fall within the range of applied pressure that could hold an ear without malformation [32, 33].

Biocompatibility is a subject that is also covered by a prosthesis because of their permanent contact with the skin or any other organ. That is why a PVDF prosthesis is ideal to prevent exposure to hazardous substances. This polymer has been used in many other kinds of biocompatible applications, and it has been widely studied as a safety material for biomedical applications [34, 35]. By the other hand, using a 3D printer, a functional ear prosthesis could be fabricated in a few hours with all the advantages mentioned above.

5. Conclusions

In this work, a prosthesis made of PVDF was manufactured satisfactorily with a 3D printer. It was also tested as pressure and temperature sensors. The characterization could be achieved satisfactorily. As shown in **Figures 7** and **8**, the typical response of the PVDF pressure and temperature sensors was found to be very reliable. It was seen that PVDF displayed a high sensitivity to pressure changes in the range 0–16.35 kPa.

Smart PVDF prostheses provide a promising tool for measuring pressure and temperature variations due to its ferroelectric properties (piezoelectricity and pyroelectricity) [5, 36]. These kind of smart prostheses have great potentialities in the biomedical engineering field because of their ability to generate an electrical potential in response to applied mechanical stress or variations of temperature, as well as flexibility [37].

Besides this, the prosthesis has displayed to be not only a reliable temperature and pressure sensor but also an acoustic one [31, 38]. This is a quite important characteristic due to the fact that the outer ear collects sound waves and channels them into the ear canal where the sound is amplified.

The light response was also satisfactory of the PVDF coinciding with the photopyroelectric techniques reported [11–13].

Finally, it is possible to manufacture sensors for TSPL based on PVDF with their respective feedback, that is, TSPL responses proportionate electrical stimulation of skin sensory nerves.

http://dx.doi.org/10.5772/63074

Acknowledgements

Authors express their gratitude to the Mexican National Council for Science and Technology (CONACYT) for financing this book chapter through the Project 151894.

Author details

Ernesto Suaste-Gómez*, Grissel Rodríguez-Roldán, Héctor Reyes-Cruz and Omar Terán-Jiménez

*Address all correspondence to: esuaste@cinvestav.mx

Department of Electrical Engineering, Section of Bioelectronics, Center for Research and Advanced Studies, Mexico City, DF, Mexico

References

[1] C. Park, Y.-S. Yoo, and S.-T. Hong. An update on auricular reconstruction: three major auricular malformations of microtia, prominent ear and cryptotia. Current Opinion in Otolaryngology & Head and Neck Surgery. 2010;18(6):544–549.

[2] G. E. Scoto-Mora, C. O. Gonzalez-Moran, and E. Suaste-Gomez. Development of poly(vinylidene flouride) polymer applied in force sensors for gait analysis in Wistar mice of physiology research laboratory. Japanese Journal of Applied Physics. 2008;47(6):4769–4771.

[3] H. R. Gallantree. Review of transducer applications of polyvinylidene fluoride. IEE Proceedings-I Communications Speech and Vision. 1983;130(5):219–224.

[4] P. Ueberschlag. PVDF piezoelectric polymer. Sensor Review. 2001;21(2):118–126.

[5] J. S. Lee, K.-Y. Shin, O. J. Cheong, J. H. Kim, and J. Jang. Highly sensitive and multi-functional tactile sensor using free-standing ZnO/PVDF thin film with graphene electrodes for pressure and temperature monitoring. Scientific Reports. 2015;5:1–8. doi: 10.1038/srep07887

[6] C. O. G. Moran, R. G. Ballesteros, M. Guzman, and E. S. Gomez. Polyvinylidene flouride polymer applied in an intraocular pressure sensor. Japanese Journal of Applied Physics Part 2-Letters & Express Letters. 2005;44(24–27):L885–L887.

[7] A. J. Lovinger. Ferroelectric polymers. Science. 1983;220:1115–1121.

[8] C. O. González-Morán, G. A. Zamora Pérez, and E. Suaste-Gómez. System for controlling the moisture of the soil using humidity sensors from a polyvinylidene fluoride fiber mats. Advanced Science Letters. 2013;19:858–861.

[9] J. S. Harrison and Z. Ounaies. Piezoelectric polymers. NASA/CR–2001–211422. 2001;2001(43). pp. 1–26.

[10] S. N. Fedosov, A. V. Sergeeva, J. A. Giacometti, and P. A. Ribeiro. Corona poling of a ferroelectric polymer (PVDF). In: A. Wlochowicz, editor. SPIE 4017, Polymers and Liquid Crystals; Szczyrk, Poland. 1999. doi:10.1117/12.373719

[11] J. A. Balderas and A. Mandelis. New technique for precise measurements of the thermal effusivity of transparent liquids. International Journal of Thermophysics. 2003;24(2): 463–471.

[12] A. Mandelis and C. Wang. A novel PVDF thin-film photopyroelectric thermal-wave interferometry. Ferroelectrics. 2000;236:235–246.

[13] G. Lara-Hernandez, A. Cruz-Orea, E. Suaste-Gomez, and J. J. A. Flores-Cuautle. Comparative performance of PLZT and PVDF sensors used phyroelectric to the thermal characterization of liquid samples. Advances in Materials Science and Engineering. 2013;2013:Article ID 281279.

[14] G.T. Davis. Piezoelectric and pyroelectric polymers. In: C. P. Wong, editor. Polymers for Electronic and Photonic Applications. Academic Press, Boston: 1993. p. 435.

[15] G. Casar, X. Li, J. Koruza, Q. Zhang, and V. Bobnar. Electrical and thermal properties of vinylidene fluoride–trifluoroethylene-based polymer system with coexisting ferroelectric and relaxor states. Journal of Materials Science. 2013;48:7920–7926.

[16] E. Jafer and K. Arshak. The use of PE/PVDF pressure and temperature sensors in smart wireless sensor network for environmental monitoring system developed. Sensor Letters. 2008;6(4):1–13.

[17] Y. Jia, Q. Ni, X. Chen, C. Ju, K. Xing, and T. Jin. Simulation and experiment of PVDF temperature sensor. Applied Mechanics and Materials. 2013;303–306:109–113.

[18] R. Z. Gan, B. Feng, and Q. Sun. Three-dimensional finite element modeling of human ear for sound transmission. Annals of Biomedical Engineering. 2004;32(6):847–859.

[19] C. Sforza, G. Grandi, M. Binelli, D. G. Tommasi, R. Rosati, and V. F. Ferrario. Age- and sex-related changes in the normal human ear. Forensic Science International. 2009;187(1–3):110.e1–110.e7.

[20] L. Ciocca, R. Mingucci, G. Gassino, and R. Scotti. CAD/CAM ear model and virtual construction of the mold. Journal of Prosthetic Dentistry. 2007;98(5):339–343.

[21] C. N. Kahue, M. L. Carlson, J. A. Daugherty, D. S. Haynes, and M. E. Glasscock III. Middle ear implants for rehabilitation of sensorineural hearing loss: a systematic review of FDA approved devices. Otology & Neurotology. 2014;35(7):1228–1237.

[22] J. R. Tysome, R. Moorthy, A. Lee, D. Jiang, and A. F. O'Connor. Systematic review of middle ear implants: do they improve hearing as much as conventional hearing aids? Otology & Neurotology. 2010;31(9):1369–1375.

[23] M. D. Wolframm, J. M. Opie, and C. Muehloecker. Active middle ear implants (AMEIs) in patients with mixed or conductive hearing losses—a review and analysis of the literature. Hearing Research. 2010;263(1–2):246.

[24] W. Buyens, B. van Dijk, J. Wouters, and M. Moonen. A stereo music preprocessing scheme for cochlear implant users. IEEE Transactions on Biomedical Engineering. 2015;62(10):2434–2442.

[25] H. D. D'Alessandro, R. Filipo, D. Ballantyne, G. Attanasio, E. Bosco, M. Nicastri, and P. Mancini. Low-frequency pitch perception in children with cochlear implants in comparison to normal hearing peers. European Archives of Oto-Rhino-Laryngology. 2015;272(11):3115–3122.

[26] A. Farinetti, S. Roman, J. Mancini, K. Baumstarck-Barrau, R. Meller, J. P. Lavieille, and J. M. Triglia. Quality of life in bimodal hearing users (unilateral cochlear implants and contralateral hearing aids). European Archives of Oto-Rhino-Laryngology. 2015;272(11):3209–3215.

[27] A. Cox, W. Sabbagh, and D. Gault. Costal cartilage or conchal cartilage for aesthetic and structural reconstruction of lower pole ear defects. Aesthetic Surgery Journal. 2012;32(3):271–274.

[28]] J. Kiefer and R. Staudenmaier. Combined aesthetic and functional reconstruction of ear malformations. In: R. Staudenmaier, editor. Aesthetics and Functionality in Ear Reconstruction, Advances in Oto-Rhino-Laryngology. Karger AG, Basel. 2010. pp. 81–94.

[29] I. Younis, D. Gault, W. Sabbagh, and N. V. Kang. Patient satisfaction and aesthetic outcomes after ear reconstruction with a Branemark-type, bone-anchored, ear prosthesis: a 16 year review. Journal of Plastic Reconstructive and Aesthetic Surgery. 2010;63(10):1650–1655.

[30] M. S. Mannoor, Z. Jiang, T. James, Y. L. Kong, K. A. Malatesta, W. O. Soboyejo, N. Verma, D. H. Gracias, and M. C. McAlpine. 3D printed bionic ears. Nano Letters. 2013;13(6):2634–2639.

[31] J. Xu, L. M. Headings, and M. J. Dapino. High sensitivity polyvinylidene fluoride microphone based on area ratio amplification and minimal capacitance. IEEE Sensors Journal. 2015;15(5):2839–2847.

[32] C. Edwards and R. Marks. Evaluation of biomechanical properties of human skin. Clinics in Dermatology. 1995;13(4):375–380.

[33] C. Pailler-Mattei, S. Bec, and H. Zahouani. In vivo measurements of the elastic mechanical properties of human skin by indentation tests. Medical Engineering & Physics. 2008;30(5):599–606.

[34] G. Laroche, Y. Marois, R. Guidoin, M. W. King, L. Martin, T. How, and Y. Douville. Polyvinylidene fluoride (PVDF) as a biomaterial—from polymeric raw-material to monofilament vascular suture. Journal of Biomedical Materials Research. 1995;29(12): 1525–1536.

[35] I. S. Bayer, M. K. Tiwari, and C. M. Megaridis. Biocompatible poly(vinylidene fluoride)/ cyanoacrylate composite coatings with tunable hydrophobicity and bonding strength. Applied Physics Letters. 2008;93(17):173902-1–173902-3.

[36] X. Qiu. Patterned piezo-, pyro-, and ferroelectricity of poled polymer electrets. Journal of Applied Physics. 2010;108(1):011101-1–011101-19.

[37] U. Klinge, B. Klosterhalfen, A. P. Ottinger, K. Junge, and V. Schumpelick. PVDF as a new polymer for the construction of surgical meshes. Biomaterials. 202;23(16):3487–3493.

[38] Y. Wei and Q. Jianxi. Design and acoustic-structural coupling analysis of bionic microphone. Advanced Materials Research. 2013;785–786:1299–1304.